Supplement of

Speciated Atmospheric Mercury during Haze and Non-haze Days in an Inland City in China

Qianqian Hong[1,3], Zhouqing Xie[1,2,3*], Cheng Liu[1,2,3*], Feiyue Wang[4], Pinhua Xie[2,3], Hui Kang[1], Jin Xu[2], Jiancheng Wang[1], Fengcheng Wu[2], Pengzhen He[1], Fusheng Mou[2], Shidong Fan[1], Yunsheng Dong[2], Haicong Zhan[1], Xiawei Yu[1], Xiyuan Chi[1], Jianguo Liu[2]

1. School of Earth and Space Sciences, University of Science and Technology of China, Hefei, 230026, China

2. Innovation Center for Excellence in Urban Atmospheric Environment of CAS & Institute of Urban Environment of CAS, Xiamen, 361021, China

3. Key Lab of Environmental Optics & Technology, Anhui Institute of Optics and Fine Mechanics, Chinese Academy of Sciences, Hefei, 230031, China

4. Department of Environment and Geography, University of Manitoba, Winnipeg, Canada

Correspondence author:

zqxie@ustc.edu.cn (Z.Q.X.); chliu81@ustc.edu.cn (C.L.)

Calculation of the production rate of NO_2HgOH

To simplify the solution of the rate equations, we use the steady state approximation to calculate the production rate of NO_2HgOH. Based on HgOH as an intermediate product, the production rate of HgOH is equal to the removal rate of HgOH. Thus, we obtain the following equation:

$$k_1[Hg^0][OH] = k_2[HgOH] + k_3[HgOH][NO_2] \quad (1)$$

From Equation (1), the intermediate HgOH can be expressed as:

$$[HgOH] = \frac{k_1[Hg^0][OH]}{k_2 + k_3[NO_2]} \quad (2)$$

The production rate of NO_2HgOH can be expressed as:

$$\frac{d[NO_2HgOH]}{dt} = k_3[HgOH][NO_2] \quad (3)$$

Substituting Eq. (2) into Eq. (3), we obtain Eq. (4) as follows:

$$\frac{d[NO_2HgOH]}{dt} = \frac{k_1k_3[Hg^0][OH][NO_2]}{k_2 + k_3[NO_2]} \quad (4)$$

In this case, rate coefficient settings are: $k_1 = 3.2\times10^{-13}$ cm^3 $molecule^{-1}$ s^{-1}, $k_2 = 3.2\times10^3$ s^{-1} (Goodsite et al., 2004) and $k_3 = 2.5\times10^{-10}$ cm^3 $molecule^{-1}$ s^{-1} (Calvert and Lindberg, 2005). The concentration of the OH radical is assigned fixed values consistent with the universal level in the troposphere: $[OH] = 5\times10^6$ molecule cm^{-3}. $[Hg^0]$ is fixed at 1.2×10^7 molecule cm^{-3} (approximates to 4 ng m^{-3}). The NO_2 concentration is changing, starting at 0 ppb and increase to several ppm (1ppb = 2.46×10^{10} molecule cm^{-3}).

Unit conversion

The mean DSCDs of NO_2 observed during the monitoring period can be converted to mixing ratios. Assuming that the trace gases were homogeneous within the 500 m height of the boundary. Mixing ratios can be calculated as (Lee et al., 2008):

$$M(\text{ppb}v) = 1.25 \times \frac{DSCD(molecule\ cm^{-2})}{dAMF} \times \frac{1}{2.688 \times 10^{16}(molecule\ DU^{-1})} \times \frac{1}{\Delta P(atom)} \quad (5)$$

where M is the mixing ratio, DSCD is the difference between the SCDs of the measured spectrum and that of the Fraunhofer reference spectrum, dAMF is a differential air mass factor (AMF(α=30°)-AMF(α=90°)), and ΔP is the pressure difference between surface and 500 m height of boundary layer, which was determined to be 0.057875 from US standard atmosphere, 1976 (Atmosphere, 1976) (http://www.digitaldutch.com/atmoscalc/index.htm).

Identification of mercury sources via HYSPLIT Trajectory model during heavy pollution events

In this study, 5-day back-trajectories were calculated in ensemble forms which calculate 27 trajectories from a selected starting point (Fig. S9). The trajectory ensemble option will start multiple trajectories from the first selected starting location. Each member of the trajectory ensemble is calculated by offsetting the meteorological data by a fixed grid factor (one grid meteorological grid point in the horizontal and 0.01 sigma units in the vertical) for the selected starting point (31.52N,117.17E) (Fain et al., 2009).

Table S1. Period of heavy pollution events and the associated GEM concentration

Events	Start Time (UTC + 8 hr)	End Time (UTC + 8 hr)	Duration (h)	Mean GEM (ng m^{-3})
1	2013/8/24 0:00	2013/8/25 13:05	37	7.88 ±1.34
2	2013/8/29 0:05	2013/8/31 3:30	51	9.58 ±3.09
3	2013/9/12 6:25	2013/9/13 9:35	27	7.98 ±1.02
4	2013/11/21 9:15	2013/11/22 12:20	27	9.46 ±1.81
5	2013/12/4 9:35	2013/12/9 12:10	123	8.40 ±1.36
6	2014/3/17 12:25	2014/3/18 21:05	33	9.77 ±2.28
7	2014/6/28 22:40	2014/6/30 1:40	27	7.86 ±1.40

Notes: these heavy pollution events were identified using the following criteria: the duration of elevated GEM concentration lasted for >24h; the elevated GEM concentration was defined as higher than 90th percentile value (6.4 ng m^{-3}).

Table S2. Rate coefficient related to the Hg reaction with OH radical in the presence of NO_2

Reaction	Rate constant (1 atm, 298K)	Reference
(R1) $Hg^0+OH \rightarrow HgOH$	$k_1=3.2\times10^{-13}$ $cm^3 molecule^{-1}s^{-1}$	Goodsite et al.(2004)
(R2) $HgOH \rightarrow Hg^0+OH$	$k_2=3.2\times10^{3}$ s^{-1}	Goodiste et al.(2004)
(R3) $HgOH+NO_2 \rightarrow NO_2HgOH$	$k_3=2.5\times10^{-10}$ $cm^3 molecule^{-1}s^{-1}$	Calvert and Lindberg et al.(2005)

Notes: k_1 and k_2 refer to the theoretical estimates of Goodsite et al. (2004).

$k(Hg+OH \rightarrow HgOH, 180\text{-}400K)=3.2\times10^{-13}(T/298K)^{-3.06}$ cm^3 $molecule^{-1}s^{-1}$

$k(HgOH \rightarrow Hg+OH, 180\text{-}400K)=2.7\times10^{9}\exp(-4061/T)$ s^{-1}

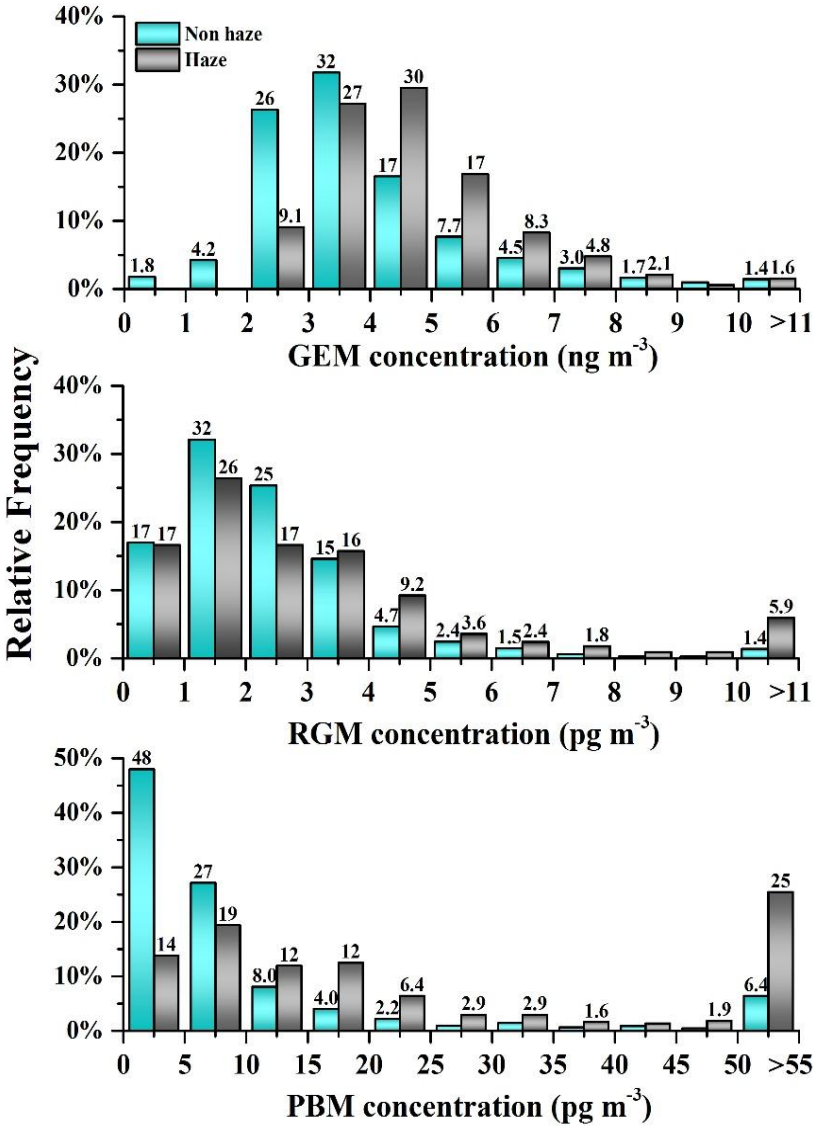

Fig. S1. Frequency distribution of GEM, RGM and PBM during the non-haze and haze days.

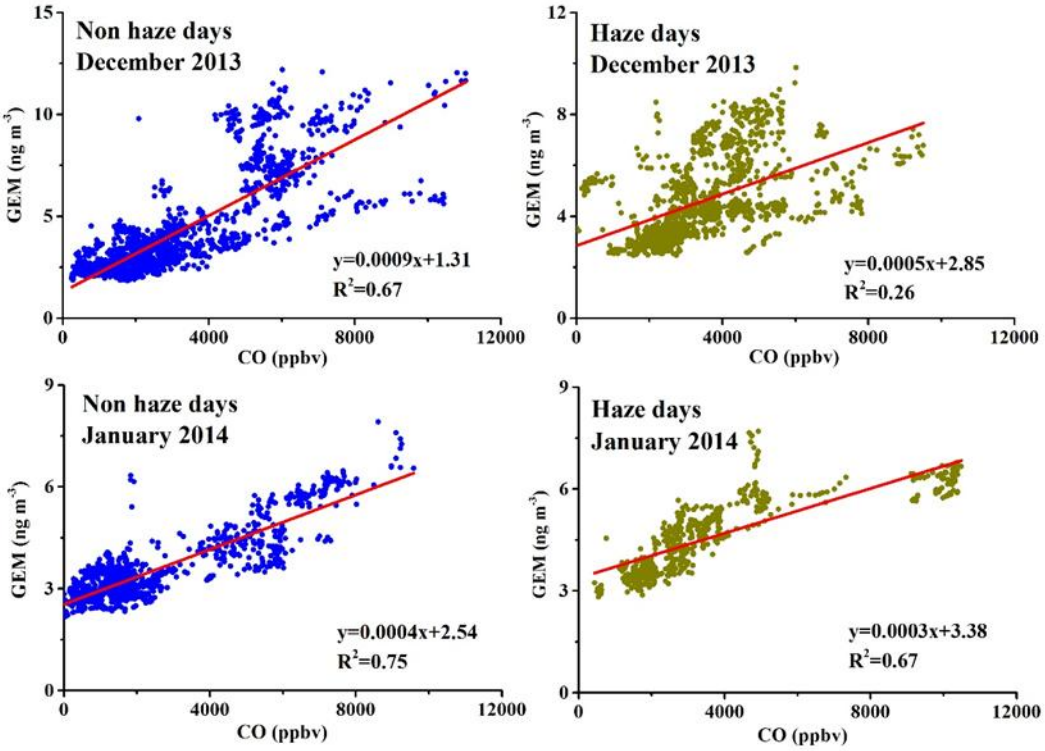

Fig. S2. Correlation between CO concentration and GEM concentration during non-haze and haze days for December 2013 and January 2014.

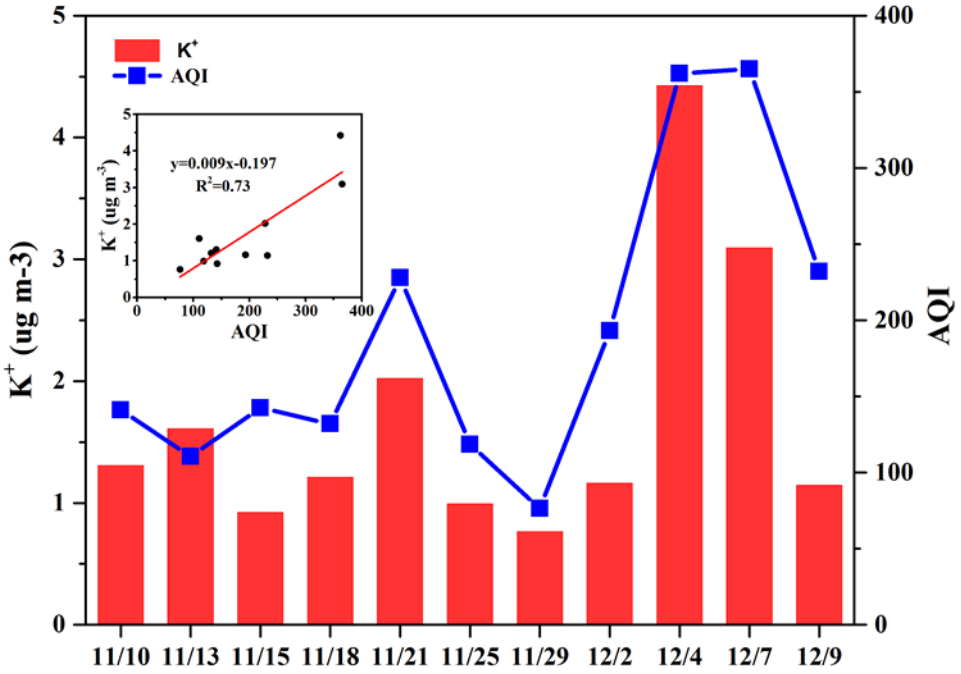

Fig. S3. Correlation between water-soluble potassium (K+) and air quality index (AQI) during heavy pollution periods (from 10 Nov to 9 Dec, 2013).

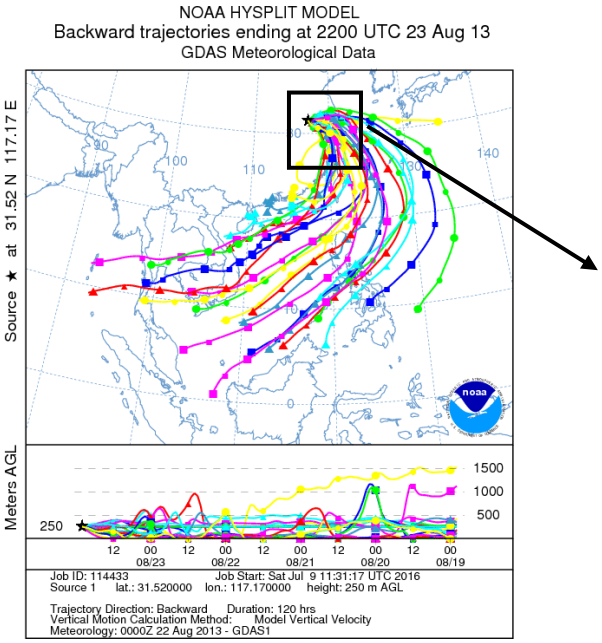

Event #1

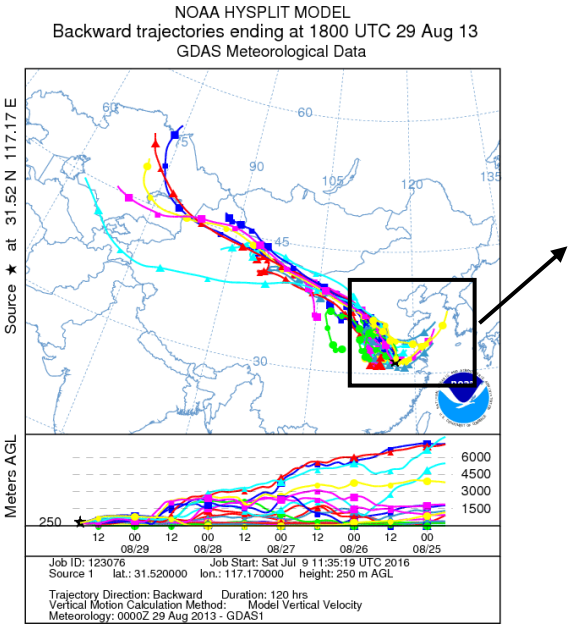

Event #2

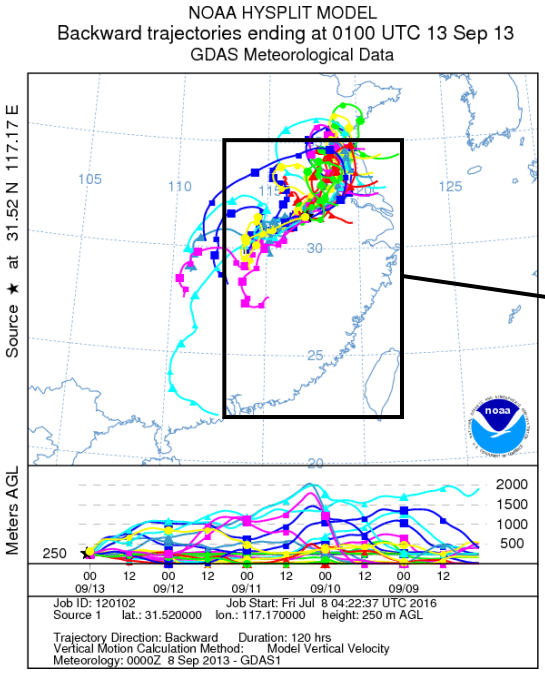

Event #3

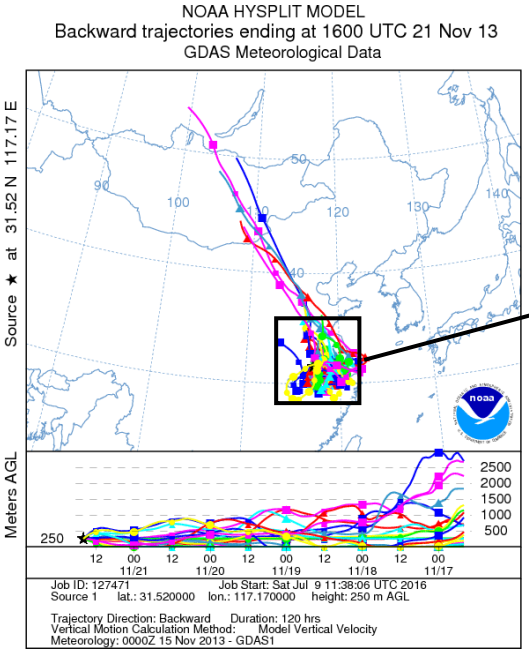

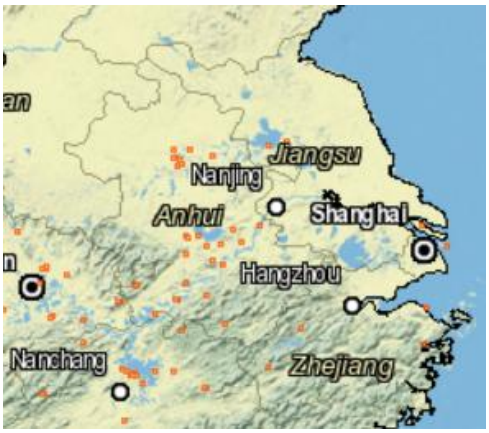

Event #4

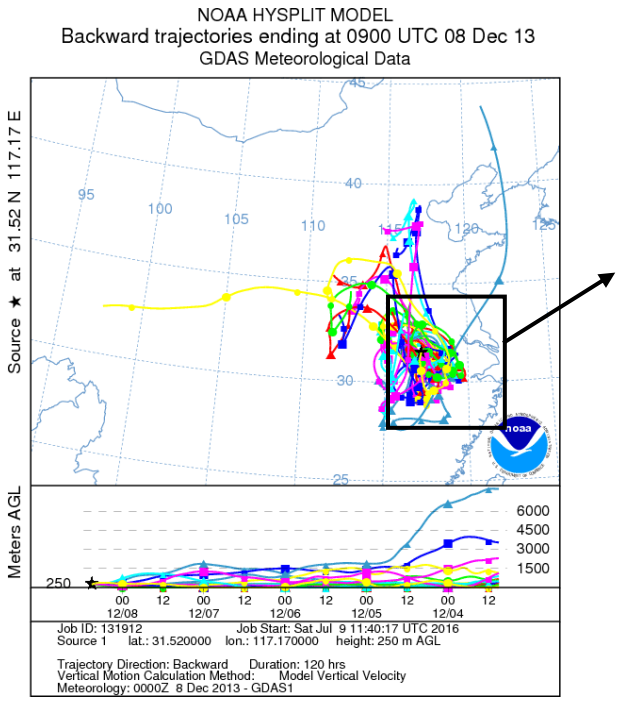

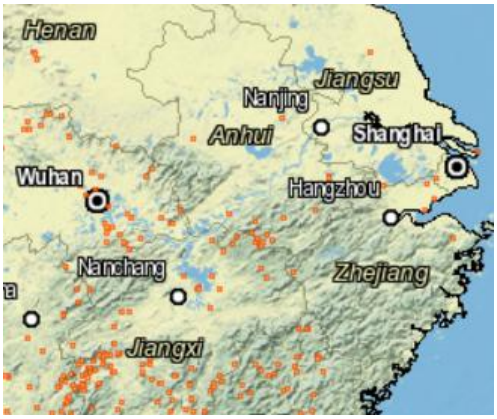

Event #5

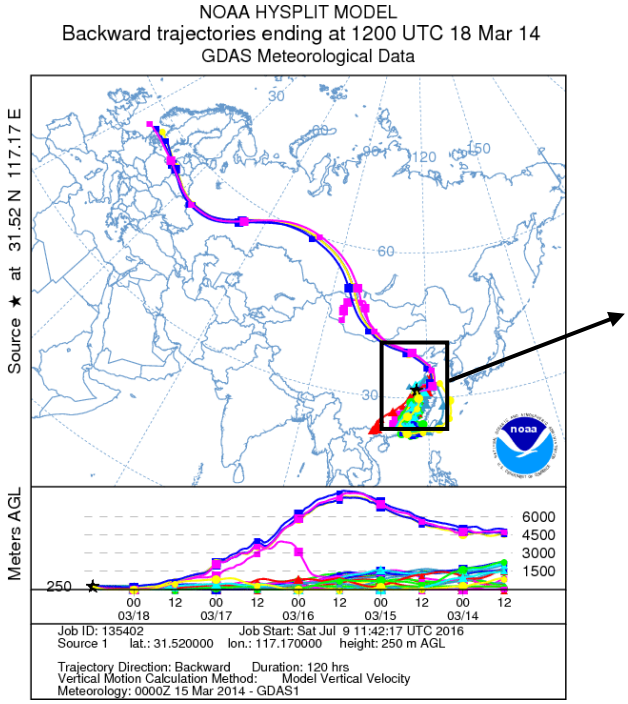

Event #6

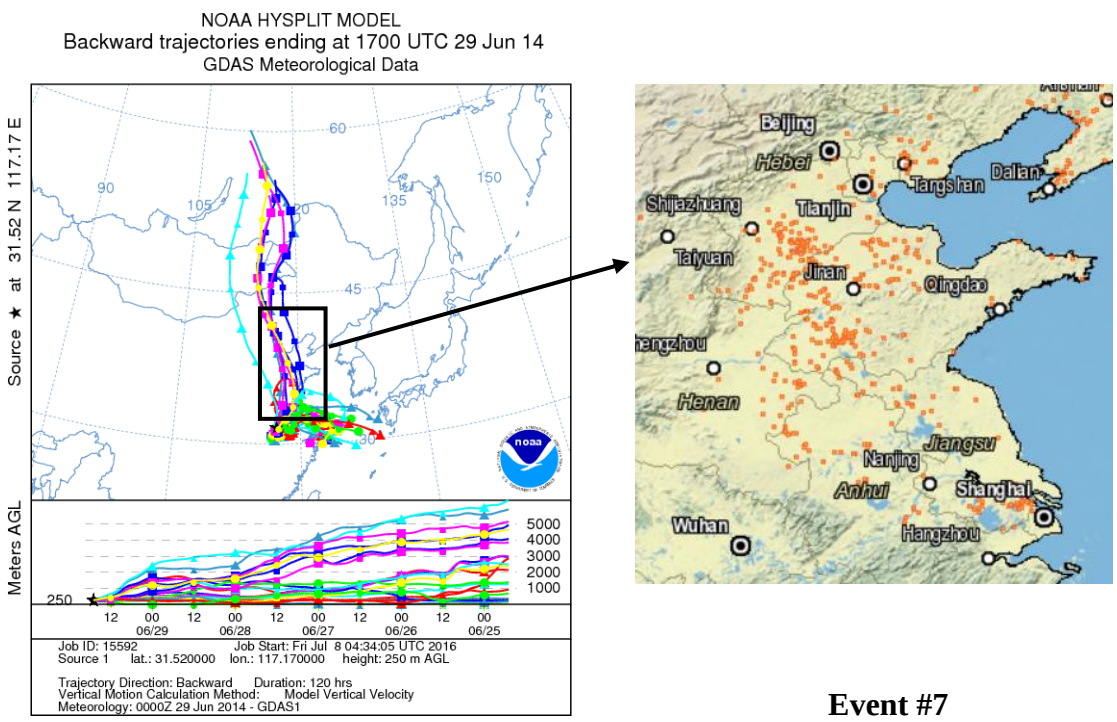

Event #7

Fig. S4. 5-days HYSPLIT air mass trajectories selected for each GEM heavy pollution event for the time of at maximum GEM concentration (left panel). Biomass burning information from FIRMS were inserted for each event (right panel).

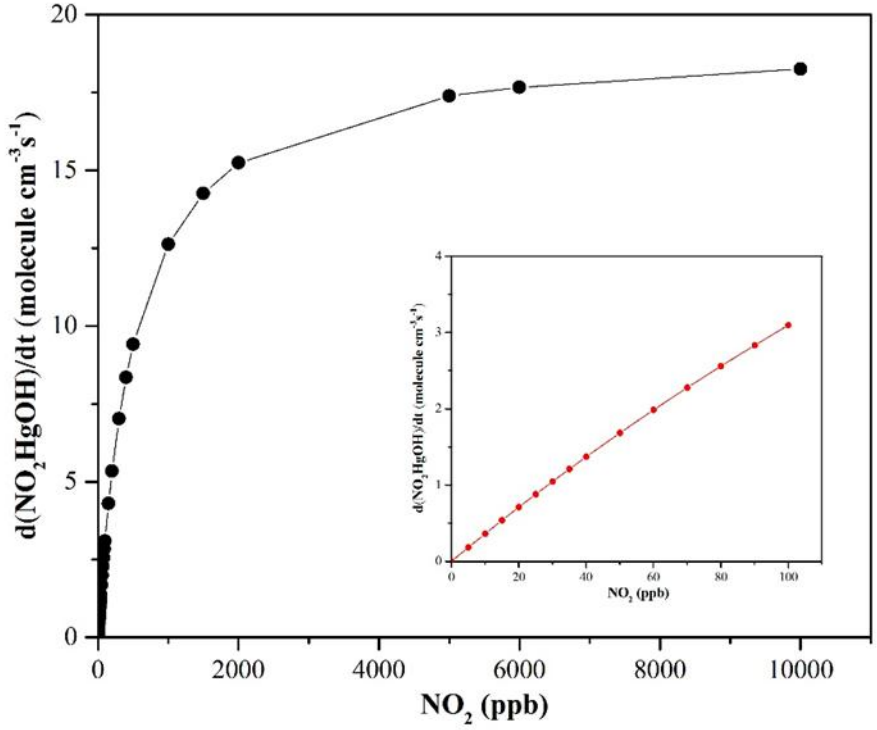

Fig. S5. The production rate of NO2HgOH (d[NO2HgOH]/dt) in response to the change of NO2.

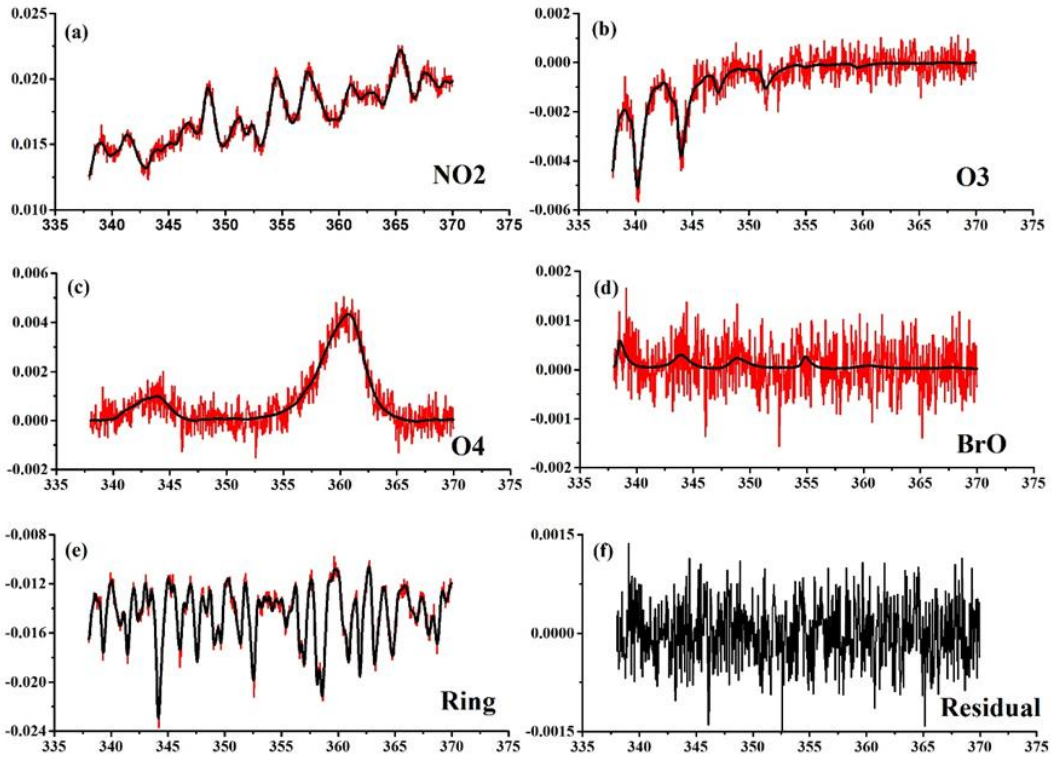

Fig. S6. An Example of the NO2 retrieval (at 30 °elevation angle) taken at 12:25 BJT (=UTC+8 hr) on 2 January 2014, with NO2 differential slant column density (DSCD) of 3.58×1016 molecules cm-2. The black lines represent the reference spectrum scaled to (a) NO2, (b) O3, (c) O4, (d) BrO, (e) Ring absorptions (red lines). The difference between measured spectrum and fit results is shown on (f) residual.

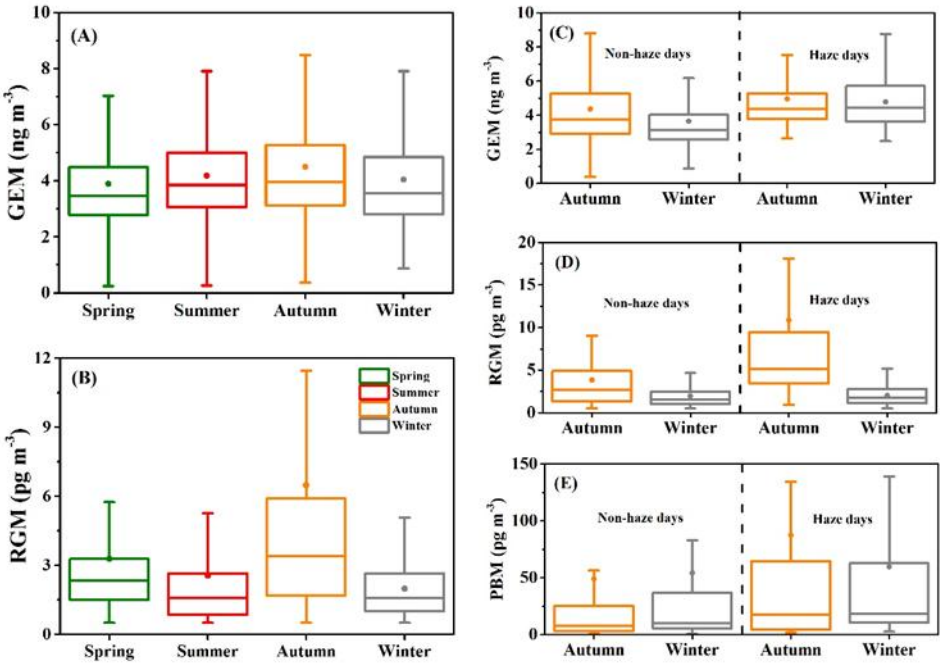

Fig. S7. Seasonal variation of (A) GEM, (B) RGM and (C&D) PBM concentrations in ambient air at Hefei, Science Island. Notes: the bottom and top of the box represent the 25th and 75th percentiles, respectively; the line within the box represent the median; the dot represents the mean; the whiskers below and above the box stands for the 10th and 90th percentiles.

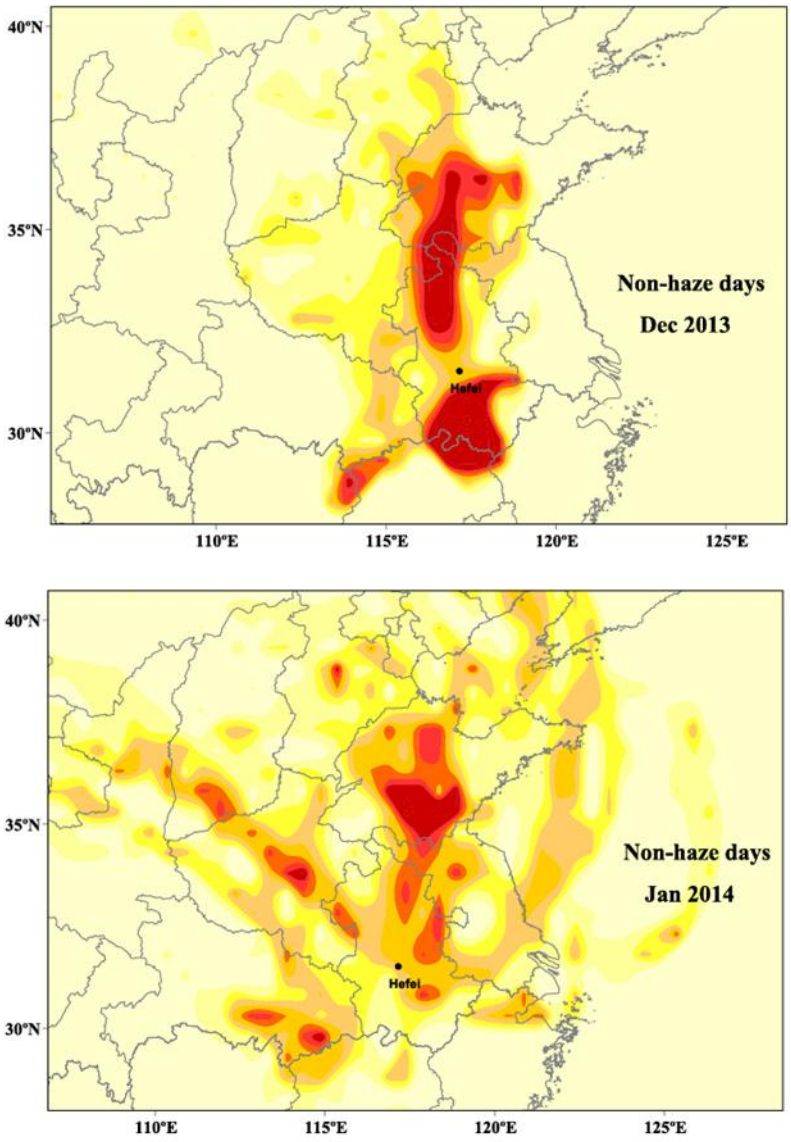

Fig. S8. Likely sources areas of GEM identified using PSCF analysis during non-haze days.

References

Atmosphere, U. S.: NASA TM-X 74335. National Oceanic and Atmospheric Administration, National Aeronautics and Space Administration and United States Air Force, 1976.

Calvert, J. G., and Lindberg, S. E.: Mechanisms of mercury removal by O_3 and OH in the atmosphere, Atmospheric Environment, 39, 3355-3367, 2005.

Fain, X., Obrist, D., Hallar, A., Mccubbin, I., and Rahn, T.: High levels of reactive gaseous mercury observed at a high elevation research laboratory in the Rocky Mountains, Atmospheric Chemistry and Physics, 9, 8049-8060, 2009.

Goodsite, M. E., Plane, J., and Skov, H.: A theoretical study of the oxidation of Hg^0 to $HgBr_2$ in the troposphere, Environmental science & technology, 38, 1772-1776, 2004.

Lee, C., Richter, A., Lee, H., Kim, Y. J., Burrows, J. P., Lee, Y. G., and Choi, B. C.: Impact of transport of sulfur dioxide from the Asian continent on the air quality over Korea during May 2005, Atmospheric Environment, 42, 1461-1475, 2008.